Appl. Math. and Comp. Sci., 1997, Vol.7, No.2, 293–303

AN ADAPTIVE FORCE/POSITION CONTROL SCHEME FOR ROBOT MANIPULATORS

STEFANO CHIAVERINI*, BRUNO SICILIANO* , LUIGI VILLANI*

An adaptive control scheme is proposed for controlling both the force and position for a robot manipulator in contact with a compliant surface. The controller is developed in the framework of parallel control of inverse-dynamics type. Adaptation to unknown stiffness is achieved by resorting to a suitable estimate update law driven by the force error. The stability of the system is formally proved, which ensures the tracking of both the position along the unconstrained directions and the force along the constrained direction. Simulation results are presented to show the applicability of the technique to practical manipulation tasks involving interaction with the environment.

1. Introduction

When the end-effector of a robot manipulator comes into contact with the environment, purely position control schemes often fail. A successful completion of interaction tasks should then be entrusted to the adoption of control strategies which make explicit use of contact force measurements (Whitney, 1987).

Well-established frameworks for controlling the interaction include impedance control (Hogan, 1985), hybrid control (Raibert and Craig, 1981), inner/outer control (De Schutter and Van Brussel, 1988), and parallel control (Chiaverini and Sciavicco, 1993). A common denominator of all these approaches is that a certain degree of knowledge about the geometry as well as the stiffness of the contact has to be provided with various implications for the particular framework.

In all practical manipulation tasks, exact knowledge of the contact stiffness cannot be ensured and the controller is typically tuned on the basis of its best available estimate. Consequently, previous research efforts have been devoted to designing control schemes with stiffness adaptation (Carelli *et al.*, 1990; Lozano and Brogliato, 1992; Yao *et al.*, 1994; Singh and Popa, 1995).

Parallel control constitutes an effective framework to handle scarce knowledge of contact geometry. Besides the original inverse dynamics controller (Chiaverini and Sciavicco, 1993), a force/position regulator (Chiaverini *et al.*, 1994) and a passivity-based controller (Siciliano and Villani, 1996) have been developed. The common feature of all these schemes is the possibility of regulating the contact force to a constant value without using explicit information on the constrained and unconstrained

* Dipartimento di Informatica e Sistemistica, Università degli Studi di Napoli Federico II, Via Claudio 21, 80125 Napoli, Italy, e-mail: siciliano@na.infn.it.

task directions. The key limitation preventing force tracking is the typical uncertainty as to the contact stiffness.

The aim of this paper is to present a new parallel control scheme with stiffness adaptation, which yields tracking of the contact force along the constrained task direction together with tracking of the end-effector position along the unconstrained task directions. The stability of the closed-loop system under the proposed controller is proved, which leads to simple conditions on the control parameters.

A case study is worked out which regards simulation of a practical task where uncertainty occurs about both the geometry and the stiffness contact.

2. Modelling

For the purpose of this work, a three-joint rigid robot manipulator performing a three-degree-of-freedom task is considered. Its joint-space dynamic model can be written in the well-known form

$$\boldsymbol{B}(\boldsymbol{q})\ddot{\boldsymbol{q}} + \boldsymbol{C}(\boldsymbol{q}, \dot{\boldsymbol{q}})\dot{\boldsymbol{q}} + \boldsymbol{d}(\boldsymbol{q}, \dot{\boldsymbol{q}}) + \boldsymbol{g}(\boldsymbol{q}) = \boldsymbol{u} - \boldsymbol{J}^T(\boldsymbol{q})\boldsymbol{f} \tag{1}$$

where $\boldsymbol{q}$ is the (3×1) vector of joint variables, $\boldsymbol{B}$ stands for the (3×3) symmetric inertia matrix, $\boldsymbol{C}\dot{\boldsymbol{q}}$ denotes the (3×1) vector of Coriolis and centrifugal torques, $\boldsymbol{d}$ stands for the (3×1) vector of friction torques, $\boldsymbol{g}$ is the (3×1) vector of gravitational torques, $\boldsymbol{u}$ stands for the (3×1) vector of driving torques, $\boldsymbol{f}$ is the (3×1) vector of contact forces exerted by the end-effector on the environment, and $\boldsymbol{J}$ denotes the (3×3) Jacobian relating joint velocities $\dot{\boldsymbol{q}}$ to the (3×1) vector of end-effector velocities $\dot{\boldsymbol{p}}$, i.e.

$$\dot{\boldsymbol{p}} = \boldsymbol{J}(\boldsymbol{q})\dot{\boldsymbol{q}} \tag{2}$$

The environment is modelled as a frictionless and elastically compliant plane. A point contact is considered and the contact force is expressed as

$$\boldsymbol{f} = \boldsymbol{K}(\boldsymbol{p} - \boldsymbol{p}_0) \tag{3}$$

where $\boldsymbol{p}$ is a (3×1) vector representing the end-effector position at the contact point, $\boldsymbol{p}_0$ stands for a (3×1) constant vector characterizing the rest position of the plane, and $\boldsymbol{K}$ is the (3×3) constant, symmetric and positive-semidefinite stiffness matrix. The assumed contact model requires that $\boldsymbol{f}$ be normal to the plane; this implies that the rank of the stiffness matrix must be one. Note that eqn. (3) holds only when the end-effector is in contact with the environment and all quantities are expressed in a common reference frame.

It is worth considering the rotation matrix expressing the orientation of the contact frame with respect to the reference frame:

$$\boldsymbol{R} = [\boldsymbol{t}_1 \quad \boldsymbol{t}_2 \quad \boldsymbol{n}] \tag{4}$$

where $\boldsymbol{n}$ is the unit vector normal to the contact plane, and $\boldsymbol{t}_1, \boldsymbol{t}_2$ are two orthogonal unit vectors lying in the plane. Projection of a vector $\boldsymbol{v}$ on the frame $\boldsymbol{R}$ gives

$$\boldsymbol{R}^T\boldsymbol{v} = \begin{bmatrix} v_{t_1} \\ v_{t_2} \\ v_n \end{bmatrix} \tag{5}$$

In view of (4), the stiffness matrix can be written as

$$\boldsymbol{K} = \boldsymbol{R}\,\mathrm{diag}\{0, 0, k\}\boldsymbol{R}^T = k\,\boldsymbol{n}\boldsymbol{n}^T \tag{6}$$

where $k > 0$ is the stiffness coefficient. It is easily seen that eqn. (6) leads to the following expression for the contact force:

$$\boldsymbol{f} = k\,\boldsymbol{n}\boldsymbol{n}^T(\boldsymbol{p} - \boldsymbol{p}_0) \tag{7}$$

3. Parallel Control

An inverse-dynamics control law can be chosen as (Sciavicco and Siciliano, 1996)

$$\begin{aligned} \boldsymbol{u} = \boldsymbol{B}(\boldsymbol{q})\boldsymbol{J}^{-1}(\boldsymbol{q})\big(\boldsymbol{a} - \dot{\boldsymbol{J}}(\boldsymbol{q}, \dot{\boldsymbol{q}})\dot{\boldsymbol{q}}\big) + \boldsymbol{C}(\boldsymbol{q}, \dot{\boldsymbol{q}})\dot{\boldsymbol{q}} + \boldsymbol{d}(\boldsymbol{q}, \dot{\boldsymbol{q}}) \\ + \boldsymbol{g}(\boldsymbol{q}) + \boldsymbol{J}^T(\boldsymbol{q})\boldsymbol{f} \end{aligned} \tag{8}$$

where $\boldsymbol{J}$ is assumed to be non-singular.

On the assumption of perfect dynamic compensation and exact force cancellation, substituting control (8) into model (1) and taking the time derivative of (2) gives a linear decoupled system expressing a resolved end-effector acceleration. System (1) under control (8) can be expressed as

$$\ddot{\boldsymbol{p}} = \boldsymbol{a} \tag{9}$$

Let $\boldsymbol{p}_d$ and $\boldsymbol{f}_d$ denote the desired values of position and force, respectively. Furthermore, let $\tilde{\boldsymbol{p}} = \boldsymbol{p}_d - \boldsymbol{p}$ and $\tilde{\boldsymbol{f}} = \boldsymbol{f}_d - \boldsymbol{f}$ denote respectively the position and force errors.

The elastic contact model (7) suggests that a null force error can be obtained only if $\boldsymbol{f}_d = f_{d,n}\boldsymbol{n}$. If no information about the geometry of the environment is available, i.e. the direction of $\boldsymbol{n}$ is unknown, the null vector can be assigned to $\boldsymbol{f}_d$ that is anyhow in the range space of any matrix $\boldsymbol{K}$. Analogously, it is clear that null position errors can be obtained only on the contact plane, while the component of $\boldsymbol{p}$ along $\boldsymbol{n}$ has to accommodate the force requirement specified by $\boldsymbol{f}_d$. Thus $\boldsymbol{p}_d$ can be freely reached only in the null space of $\boldsymbol{K}$, i.e. along the unconstrained directions of the task space.

By following the parallel control approach, the new control input $\boldsymbol{a}$ is designed as the sum of a position control action and a force control action (Chiaverini and Sciavicco, 1988):

$$\boldsymbol{a} = \boldsymbol{a}_p + \boldsymbol{a}_f \tag{10}$$

where the force control action will dominate the position control action along the constrained task direction.

The classical design is to take $\boldsymbol{a}_p$ as a PD action on the position error plus velocity and desired acceleration feedforward, and $\boldsymbol{a}_f$ as a PI action on the force error plus desired force feedforward (Chiaverini and Sciavicco, 1993). This choice ensures dominance of the force loop over the position loop in that a null force error can be achieved at the expense of a constant position error in the steady state. Nevertheless, the choice of the parameters for the force loop depends on the choice of the parameters for the position loop, and stability of a third-order linear system has to be guaranteed.

A modified design consists in taking the force control action in such a way as to cancel the dynamics imposed by the position control action and replace it with a new second-order dynamics. An integral action on the force error has still to be adopted in order to obtain the null force error in a steady state. This has the advantage of making the force control loop design independent of the position control loop design (Chiaverini *et al.*, 1996). Therefore the two control actions in (8) are taken as:

$$\boldsymbol{a}_p = \ddot{\boldsymbol{p}}_d + k_D\dot{\tilde{\boldsymbol{p}}} + k_P\tilde{\boldsymbol{p}} \tag{11}$$

$$\boldsymbol{a}_f = \ddot{\boldsymbol{\xi}} + k_D\dot{\boldsymbol{\xi}} + k_P\boldsymbol{\xi} \tag{12}$$

where $k_P, k_D > 0$ are suitable control parameters to impose the desired dynamics on the position, and $\boldsymbol{\xi}$ is the solution of

$$\ddot{\boldsymbol{\xi}} + \lambda_2\dot{\boldsymbol{\xi}} = \lambda_1\tilde{\boldsymbol{f}} \tag{13}$$

for given initial conditions $\boldsymbol{\xi}(0)$, $\dot{\boldsymbol{\xi}}(0)$; $\lambda_1, \lambda_2 > 0$ are suitable control parameters to impose the desired dynamics on the force.

Following the guidelines in (Chiaverini and Sciavicco, 1993), it is possible to analyze the behaviour of system (9)–(13) by projecting its dynamics in terms of contact plane components along $\boldsymbol{t}_1$, $\boldsymbol{t}_2$, and the component along $\boldsymbol{n}$. In detail, it is obvious that if $\boldsymbol{f}_d$ is along $\boldsymbol{n}$, system (9)–(13) ensures the position reference trajectory along the contact plane components. On the other hand, it can be recognized that $\boldsymbol{f}$ tends to a constant set point $\boldsymbol{f}_d$ in a steady state—when $\boldsymbol{p}_d$ is constant along $\boldsymbol{n}$—with a dynamics depending on the stiffness coefficient k, for any given λ_1 and λ_2. In other words, regulation of the contact force is achieved.

To improve the performance of the force loop during the transient and eventually achieve contact force tracking capabilities, knowledge of the stiffness coefficient must be included into the control law. The needed compensation actions can be either tuned on the basis of the value of the stiffness coefficient whenever available, or driven by an adaptive algorithm when stiffness is not exactly known *a priori*. For this purpose, eqn. (13) must be replaced with

$$\ddot{\boldsymbol{\xi}} + \lambda_2\dot{\boldsymbol{\xi}} = \lambda_1\boldsymbol{f}_c \tag{14}$$

in which the new control input $\boldsymbol{f}_c$ should be properly designed.

In view of the above discussion, in the sequel it is assumed that $\boldsymbol{f}_d = f_{d,n}\boldsymbol{n}$ and $p_{d,n}$ is constant.

4. Known Stiffness

If k is known, $\boldsymbol{f}_c$ in (14) can be chosen as

$$\boldsymbol{f}_c = \frac{1}{k}\boldsymbol{\varphi} \tag{15}$$

with

$$\boldsymbol{\varphi} = \tilde{\boldsymbol{f}} + \frac{1}{\lambda_1}(\ddot{\boldsymbol{f}}_d + \lambda_2 \dot{\boldsymbol{f}}_d) \tag{16}$$

Theorem 1. *The system (1), (7) under the control law (8), (10)–(12), (14)–(16) has a globally exponentially stable equilibrium for any choice of* $k_P > 0$, $k_D > 0$, $\lambda_1 > 0$, $\lambda_2 > 0$. *In particular,* $p_{t_1} \to p_{d,t_1}$, $p_{t_2} \to p_{d,t_2}$, $f_n \to f_{d,n}$ *as* $t \to \infty$.

Proof. The system (1), (7) under the control law (8) leads to (9). Substituting (10)–(12) into (9) and projecting onto $\boldsymbol{R}$, we obtain

$$\ddot{\tilde{p}}_{t_1} + k_D \dot{\tilde{p}}_{t_1} + k_P \tilde{p}_{t_1} = 0 \tag{17}$$

$$\ddot{\tilde{p}}_{t_2} + k_D \dot{\tilde{p}}_{t_2} + k_P \tilde{p}_{t_2} = 0 \tag{18}$$

$$\ddot{\tilde{p}}_n + k_D \dot{\tilde{p}}_n + k_P \tilde{p}_n = \ddot{\xi}_n + k_D \dot{\xi}_n + k_P \xi_n \tag{19}$$

It must be pointed out that the above projection has taken (14)–(16) into account in that $\boldsymbol{\xi}$ is aligned with $\boldsymbol{n}$, being both $\boldsymbol{f}$ and $\boldsymbol{f}_d$ along $\boldsymbol{n}$.

Equations (17) and (18) imply that $p_{t_1} \to p_{d,t_1}$, $p_{t_2} \to p_{d,t_2}$ for any positive k_P, k_D and initial conditions $\tilde{p}_{t_1}(0)$, $\dot{p}_{t,1}(0)$, $\tilde{p}_{t_2}(0)$, $\dot{p}_{t,2}(0)$.

On the other hand, the solution to eqn. (19) is

$$\tilde{p}_n(t) = -\xi_n(t) + \varepsilon(t) \tag{20}$$

where $\varepsilon(t)$ is an exponentially decreasing function depending on the initial conditions $\tilde{p}_n(0)$, $\dot{p}_n(0)$.

By projecting model (7) onto $\boldsymbol{n}$, the component of the force error can be expressed as

$$\tilde{f}_n = k\tilde{p}_n + f_{d,n} + k(p_{0,n} - p_{d,n}) \tag{21}$$

Then, solving (21) with respect to $\tilde{p}_n$ and substituting the result into (20) give

$$\xi_n = -\frac{\tilde{f}_n}{k} + \frac{f_{d,n}}{k} + p_{0,n} - p_{d,n} + \varepsilon \tag{22}$$

At this point, substitution of (15), (16), and (22) into (14) gives

$$\dddot{\tilde{f}}_n + \lambda_2 \ddot{\tilde{f}}_n + \lambda_1 \dot{\tilde{f}}_n = \varepsilon' \tag{23}$$

where $\varepsilon' = k(\ddot{\varepsilon} + \lambda_2 \dot{\varepsilon})$ is an exponentially decreasing function of time. It is easy to check that $\tilde{f}_n \to 0$ as $t \to \infty$ for any positive value of λ_1, λ_2 and initial conditions $\tilde{f}_n(0)$, $\dot{\tilde{f}}_n(0)$.

The dynamics of the closed-loop system (1), (7), (8), (10)–(12), (14)–(16) is described by eqns. (17), (18), (19) and by the projection of eqns. (14)–(16) onto $\boldsymbol{n}$. On the basis of the above considerations, the state

$$[p_{t_1} \quad p_{t_2} \quad p_n \quad \xi_n \quad \dot{p}_{t_1} \quad \dot{p}_{t_2} \quad \dot{p}_n \quad \dot{\xi}_n]^T$$

converges exponentially to the equilibrium

$$[p_{d,t_1} \quad p_{d,t_2} \quad f_{d,n}/k + p_{0,n} \quad f_{d,n}/k + p_{0,n} - p_{d,n} \quad \dot{p}_{d,t_1} \quad \dot{p}_{d,t_2} \quad \dot{f}_{d,n}/k \quad \dot{f}_{d,n}/k]^T$$

from any initial condition. ■

5. Unknown Stiffness

In most practical cases, the value of the stiffness coefficient is not exactly known *a priori*. Nevertheless, an adaptive control law can be found to ensure tracking the force reference trajectory.

Inspired by the technique in (Canudas de Wit and Brogliato, 1994), the input signal $\boldsymbol{f}_c$ can be modified into

$$\boldsymbol{f}_c = \hat{\vartheta}\boldsymbol{\varphi} + \dot{\hat{\vartheta}}\bar{\boldsymbol{\varphi}} \tag{24}$$

where $\bar{\boldsymbol{\varphi}}$ is the solution of

$$\dot{\bar{\boldsymbol{\varphi}}} + \lambda_3 \bar{\boldsymbol{\varphi}} = \boldsymbol{\varphi} \tag{25}$$

with $\lambda_3 > 0$ and initial condition $\boldsymbol{\varphi}(0)$, while the estimate $\hat{\vartheta}$ is updated as

$$\dot{\hat{\vartheta}} = \gamma \bar{\boldsymbol{\varphi}}^T \tilde{\boldsymbol{f}} \tag{26}$$

with $\gamma > 0$ and initial condition $\hat{\vartheta}(0)$.

Theorem 2. *The system (1), (7) under the control law (8), (10)–(12), (24)–(26) has a stable equilibrium for any choice of* $k_P > 0$, $k_D > 0$, $\gamma > 0$, $\lambda_1 > 0$, $\lambda_2 > 0$, $\lambda_3 > \lambda_2$. *In particular,* $p_{t_1} \to p_{d,t_1}$, $p_{t_2} \to p_{d,t_2}$, $f_n \to f_{d,n}$ *as* $t \to \infty$.

Proof. Following the main ideas in the previous proof, the system (1), (7) under control law (8), (10)–(12) leads to eqns. (17)–(19). Again, (17) and (18) imply that $p_{t_1} \to p_{d,t_1}$, $p_{t_2} \to p_{d,t_2}$ for any positive k_P, k_D and initial conditions $\tilde{p}_{t_1}(0)$, $\dot{p}_{t,1}(0)$, $\tilde{p}_{t_2}(0)$, $\dot{p}_{t,2}(0)$. On the other hand, the solution to (19) leads to (22).

Equation (24) can be rewritten as

$$\boldsymbol{f}_c = \vartheta\boldsymbol{\varphi} - \tilde{\vartheta}\boldsymbol{\varphi} - \dot{\tilde{\vartheta}}\bar{\boldsymbol{\varphi}} \tag{27}$$

where $\tilde{\vartheta} = \vartheta - \hat{\vartheta}$ and $\vartheta = 1/k$. Combining (27) with (25) gives

$$\boldsymbol{f}_c = \vartheta\boldsymbol{\varphi} - \dot{\boldsymbol{\psi}} - \lambda_3 \boldsymbol{\psi} \tag{28}$$

with

$$\psi = \tilde{\vartheta}\bar{\varphi} \tag{29}$$

At this point, substitution of eqns. (16), (22), (28) and (29) into (14) gives

$$\ddot{\tilde{f}}_n + \lambda_2 \dot{\tilde{f}}_n + \lambda_1 \tilde{f}_n = k\lambda_1(\dot{\psi}_n + \lambda_3 \psi_n) + \varepsilon' \tag{30}$$

Equation (26) can be rewritten as

$$\dot{\tilde{\vartheta}} = \gamma \bar{\varphi}_n \tilde{f}_n \tag{31}$$

whereas eqn. (30) can be rewritten in the following minimal state-space form:

$$\begin{aligned} \dot{\boldsymbol{x}} &= \boldsymbol{A}\boldsymbol{x} + \boldsymbol{b}_1\psi_n + \boldsymbol{b}_2\varepsilon' \\ \tilde{f}_n &= \boldsymbol{c}^T\boldsymbol{x} \end{aligned} \tag{32}$$

with

$$\boldsymbol{A} = \begin{bmatrix} 0 & -\lambda_1 \\ 1 & -\lambda_2 \end{bmatrix} \tag{33}$$

$$\boldsymbol{b}_1 = \begin{bmatrix} k\lambda_1\lambda_3 \\ k\lambda_1 \end{bmatrix} \tag{34}$$

$$\boldsymbol{b}_2 = \begin{bmatrix} 1 \\ 0 \end{bmatrix} \tag{35}$$

$$\boldsymbol{c} = \begin{bmatrix} 0 \\ 1 \end{bmatrix} \tag{36}$$

for the state $\boldsymbol{x} = \left[\int(-\lambda_1 \tilde{f}_n + k\lambda_1\lambda_3\psi_n + \varepsilon')\,\mathrm{d}\tau \;\; \tilde{f}_n\right]^T$.

The transfer function

$$\boldsymbol{c}^T(s\boldsymbol{I} - \boldsymbol{A})^{-1}\boldsymbol{b}_1 = k\frac{\lambda_1(s+\lambda_3)}{s^2 + \lambda_2 s + \lambda_1} \tag{37}$$

can be made strictly positive real with a proper choice of the parameters λ_1, λ_2, λ_3. In particular, sufficient conditions are

$$\lambda_1 > 0 \tag{38}$$

$$\lambda_2 > 0 \tag{39}$$

$$\lambda_3 > \lambda_2 \tag{40}$$

From the Kalman-Yakubovich-Popov lemma (Khalil, 1992) it follows that there exist a symmetric positive-definite matrix $\boldsymbol{P}$ and a positive-definite matrix $\boldsymbol{Q}$ such that

$$\boldsymbol{A}^T\boldsymbol{P} + \boldsymbol{P}\boldsymbol{A} = -\boldsymbol{Q} \tag{41}$$

$$\boldsymbol{P}\boldsymbol{b}_1 = \boldsymbol{c} \tag{42}$$

Consider the function

$$V = \boldsymbol{x}^T\boldsymbol{P}\boldsymbol{x} + \frac{\tilde{\vartheta}^2}{\gamma} + \mu \int_t^\infty \varepsilon'^2(\tau)\, \mathrm{d}\tau \tag{43}$$

where $\mu > 0$ is a free parameter. Computing the time derivative of V along the trajectories of the system (31), (32) gives

$$\begin{aligned} \dot{V} &= -\boldsymbol{x}^T\boldsymbol{Q}\boldsymbol{x} + 2\tilde{f}_n\psi_n - 2\tilde{\vartheta}\bar{\varphi}_n\tilde{f}_n + 2\boldsymbol{x}^T\boldsymbol{P}\boldsymbol{b}_2\varepsilon' - \mu\varepsilon'^2 \\ &= -\boldsymbol{x}^T\boldsymbol{Q}\boldsymbol{x} + 2\boldsymbol{x}^T\boldsymbol{P}\boldsymbol{b}_2\varepsilon' - \mu\varepsilon'^2 \\ &\leq -q\|\boldsymbol{x}\|^2 + 2p\|\boldsymbol{x}\|\,|\varepsilon'| - \mu|\varepsilon'|^2 \end{aligned} \tag{44}$$

where the projection of (29) onto $\boldsymbol{n}$ has been exploited. Here $q > 0$ is the minimum eigenvalue of the matrix $\boldsymbol{Q}$, and $p > 0$ is the maximum eigenvalue of the matrix $\boldsymbol{P}$.

In view of (44), the choice $\mu > p^2/q$ ensures $\dot{V} \leq 0$. Hence $V(t)$ is a decreasing function of time. Taking into account that $V > 0$, the boundedness of $V(t)$ for any $t \geq 0$ and the convergence of $V(t)$ as $t \to \infty$ can be concluded.

On the other hand, the expression for V in (43) reveals that the boundedness of V implies that of $\boldsymbol{x}$ and $\tilde{\vartheta}$. Moreover, the boundedness of $\dot{\boldsymbol{x}}$ can be inferred from (32) through (16), (25), (29). Therefore, $\dot{V}(t)$ is bounded, too, and $\dot{V}(t)$ is uniformly continuous. From Barbalat's lemma it follows that $\dot{V}(t) \to 0$ as $t \to \infty$. Then $\boldsymbol{x} \to \boldsymbol{0}$ from (44), ε' being an exponentially decreasing function of time. Finally, in view of (32), $\tilde{f}_n \to 0$ as $t \to \infty$.

The dynamics of the closed-loop system (1), (7), (8), (10)–(12), (24)–(26) is described by eqns. (17)–(19), (31), (32). Hence, all the signals of the system are bounded and the stability can be concluded. ■

6. Simulations

Simulations have been worked out by considering an industrial robot Comau SMART-3 S which is a six-revolute-joint anthropomorphic manipulator with non-null shoulder and elbow offsets, and a non-spherical wrist. In the present study, only the inner three joints have been considered and an identified dynamic model of the manipulator has been utilized. Also, a discrete-time implementation of the control algorithm with 1 ms sampling interval has been assumed.

The task consists in a straight-line motion in the yz-plane with an end-effector (horizontal) displacement of 0.25 m along the y-axis and a (vertical) displacement

of 0.125 m along the z-axis. The trajectory along the path is generated according to a 5th-order interpolating polynomial with null initial and final velocities and accelerations, and a duration of 6 s. The environment surface is flat and is placed (horizontally) in the xy-plane in such a way as to obstruct the desired end-effector motion. To begin, a null set point is assigned to the contact force. When the end-effector comes into contact with the environment, i.e. a non-negligible force is sensed, the desired force along the z-axis is taken to -40 N according to a 5th-order polynomial with null initial and final first and second time derivatives, and a duration of 1 s. The constant value is kept for 0.5 s, and then the desired force is taken back to zero in 1 s with the same polynomial as above, making a tooth-shaped profile. After a 0.5 s lapse, the same tooth is replicated.

The above task is first executed using the control scheme described in Section 4. Obviously, inaccurate knowledge of the environment stiffness has been assumed. Therefore, uncertainty occurs as to both the geometry and the stiffness contact.

The control parameters in (11) have been set to $k_P = 2500$, $k_D = 90$ so as to guarantee well-damped behaviour for the unconstrained motion of the manipulator. Also, the control parameters in (14)–(16) have been set to $\lambda_1 = 180$, $\lambda_2 = 30$ so as to achieve satisfactory behaviour during the constrained motion with an estimated value of 10000 N/m for k. The true stiffness coefficient of the environment is $k = 5000$ N/m, instead.

The simulation results are presented in Fig. 1 in terms of the desired (dashed) and actual (solid) end-effector paths, together with the time history of the desired (dashed) and actual (solid) contact force. For the sake of clarity, the rest position of the contact plane is also depicted (dash-dotted). It can be recognized that after a transient the contact force attempts to track the given force trajectory. A peak on the component along the z-axis is due to a non-zero value of the end-effector velocity at the contact as well as to the imposed motion into the surface. When the desired force is taken back to zero, a time delay is experienced by the contact force in tracking the reference trajectory. This is mainly imputed to the mismatch of the estimated and true values of k. This time-delay effect can also be observed while tracking the second force tooth. On the other hand, the path is satisfactorily tracked before the contact. After the contact, position errors occur only along the z-axis due to the presence of the contact surface, as expected.

Next, the performance of a new controller with stiffness adaptation (described in Section 5) has been tested for the same task as above. The values of k_P, k_D, λ_1, λ_2 are the same as in the previous scheme, while the design parameters in (25) and (26) have been chosen as $\lambda_3 = 45$ and $\gamma = 0.00004$, respectively. The initial estimate $\hat{\vartheta}(0)$ has been set to 0.0001, according to the nominal stiffness value. In Fig. 2 it can be seen how the adaptation mechanism is promptly capable of ensuring contact force tracking even in the presence of a time-varying $p_{d,n}$ after the contact for the duration of the steered motion. Further, the position tracking performance is substantially unaffected by the modified controller and similar conclusions as for the previous case can be drawn.

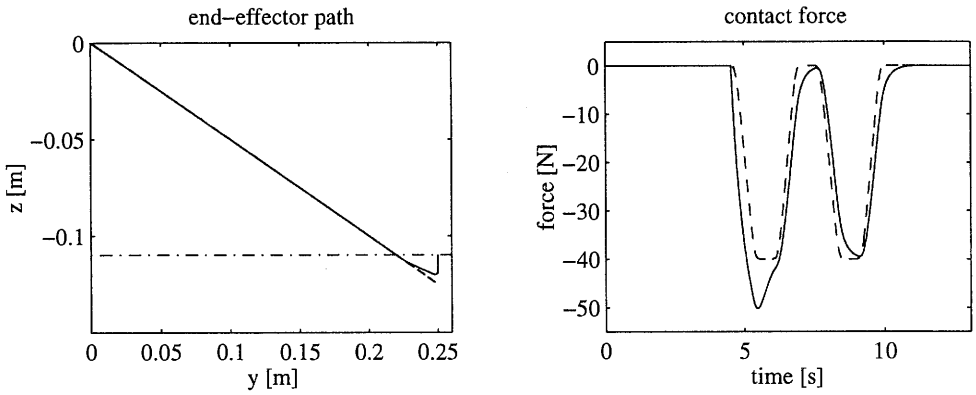

Fig. 1. Simulation results without stiffness adaptation.

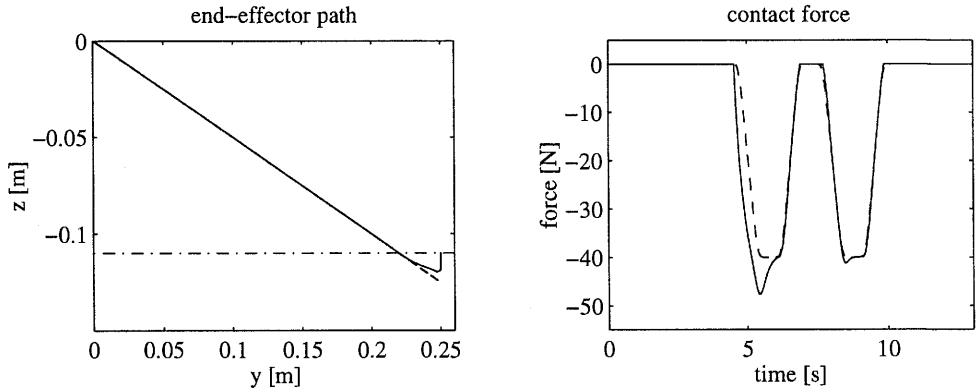

Fig. 2. Simulation results with stiffness adaptation.

7. Concluding Remarks

Parallel force/position control for a robot manipulator in contact with a compliant plane has been presented in this work. With respect to the class of the existing schemes of inverse-dynamics type, the problem of improving the contact force transient has been handled by requiring force tracking capabilities. To this end, two schemes have been considered. The first scheme has been devised assuming exact knowledge of the stiffness coefficient characterizing the contact. Then, an adaptation mechanism has been developed in the second scheme, allowing for contact force tracking when exact knowledge of the stiffness coefficient is not available. The schemes have been successfully tested in simulation to show applicability of the approach to a real interaction task.

Acknowledgements

This work was supported by Ministero dell'Università e della Ricerca Scientifica e Tecnologica under 40% and 60% funds, respectively.

References

Canudas de Wit C. and Brogliato B. (1994): *Direct adaptive impedance control.* — Postp. 4th IFAC Symp. *Robot Control*, Capri, Vol.1, pp.345–350.

Carelli R., Kelly R. and Ortega R. (1990): *Adaptive force control of robot ma- nipulators.* — Int. J. Contr., Vol.52, No.1, pp.37–54.

Chiaverini S. and Sciavicco L. (1988): *Force/position control of manipulators in task space with dominance in force.* — Postp. 2nd IFAC Symp. *Robot Control*, Karlsruhe, pp.137–143.

Chiaverini S. and Sciavicco L. (1993): *The parallel approach to force/position control of robotic manipulators.* — IEEE Trans. Robot. Automat. Vol.9, No.4, pp.361–373.

Chiaverini S., Siciliano B. and Villani L. (1994): *Force/position regulation of compliant robot manipulators.* — IEEE Trans. Automat. Contr., Vol.39, No.3, pp.647–652.

Chiaverini, S., Siciliano B. and Villani L. (1996): *Parallel force/position control schemes with experiments on an industrial robot manipulator.* — Prep. 14th IFAC World Congress, San Francisco, CA, Vol.A, pp.25–30.

De Schutter J. and Van Brussel H. (1988): *Compliant robot motion II. A control approach based on external control loops.* — Int. J. Robot. Res., Vol.7, No.4, pp.18–33.

Hogan N. (1985): *Impedance control: An approach to manipulation, Parts I–III.* — ASME J. Dyn. Systems, Meas. Contr., Vol.107, No.1, pp.1–24.

Khalil H.K. (1992): *Nonlinear Systems.* — New York: MacMillan.

Lozano R. and Brogliato B. (1992): *Adaptive hybrid force-position control for redundant manipulators.* — IEEE Trans. Automat. Contr., Vol.37, No.10, pp.1501–1505.

Raibert M.H. and Craig J.J. (1981): *Hybrid position/force control of manipulators.* — ASME J. Dyn. Systems, Meas. Contr., Vol.103, No.2, pp.126–133.

Sciavicco L. and Siciliano B. (1996): *Modeling and Control of Robot Manipulators.* — New York: McGraw-Hill.

Siciliano B. and Villani L. (1996): *A passivity-based approach to force regulation and motion control of robot manipulators.* — Automatica, Vol.32, No.3, pp.443–447.

Singh S.K. and Popa D.O. (1995): *An analysis of some fundamental problems in adaptive control of force and impedance behaviour: Theory and experiments.* — IEEE Trans. Robot. Automat., Vol.11, No.6, pp.912–921.

Whitney D.E. (1987): *Historical perspective and state of the art in robot force control.* — Int. J. Robot. Res., Vol.6, No.1, pp.3–14.

Yao B., Chan S.P. and Wang D. (1994): *Variable structure adaptive motion and force control of robot manipulators.* — Automatica, Vol.30, No.9, pp.1473–1477.